Advances and Applications in Mathematical Sciences
Volume 19, Issue 9, July 2020, Pages 833-858

DISPLACEMENT FIELD OF AN ISOTROPIC HALF-SPACE IN SMOOTH CONTACT WITH AN ORTHOTROPIC HALF-SPACE DUE TO A LONG TENSILE FAULT OF FINITE WIDTH

MINAKSHI, YOGITA GODARA, RAVINDER KUMAR SAHRAWAT and MAHABIR SINGH

Department of Mathematics
GCW, Sampla
Rohtak-124001, India

Department of Mathematics
GC, Meham
Rohtak-124001, India

Department of Mathematics
Deenbandhu Chhotu Ram
University of Science and Technology
Murthal, Sonepat-131039, India

CoE, Deenbandhu Chhotu Ram
University of Science and Technology
Murthal, Sonepat-131039, India

Abstract

Closed-form analytical expressions for displacements at any point of a two-phase medium consisting of a homogeneous, isotropic, perfectly elastic half-space in smooth contact with a homogeneous, orthotropic, perfectly elastic half-space caused by a tensile fault of finite width located at an arbitrary distance from the interface in the isotropic half-space are obtained. The Airy stress function approach is used to obtain the expressions for displacements using the stress field by Minakshi [11]. The variation of the displacement field with the distance from the fault and with depth has been studied graphically for various dip angles. The effect of depth and dip angle is also examined. Also, the horizontal and vertical displacements of the surface are depicted graphically.

2010 Mathematics Subject Classification: 74A10.
Keywords: Isotropic half-space; tensile fault; orthotropic half-space; smooth contact.
Received November 1, 2019; Accepted November 23, 2019

1. Introduction

The study of earthquakes is linked closely to various fields including Basic Sciences such as Physics and Mathematics. Generally, earthquakes occur along geological faults which are surfaces of material discontinuity in the earth. A fault may be regarded as a dislocation created by the fracture of the rock material separating two rock masses. During the fracture of the two opposing fault surfaces suffer displacement with respect to each other. Fault models can provide valuable insights into the characteristics of faults and their behavior over time. These models can provide estimates of future deformation based on the observations of the past. The basic objective of these models is to provide mathematical explanation of how Earth's crust spatially deforms and ultimately predict how it will change with time. The tensile source model is the generalization of the shear source model with the assumption that the slip vector can be arbitrarily oriented with respect to the fault and is not constrained to lie within the fault plane. In particular, tensile earthquakes occur in geothermal and volcanic areas which are rich in fluids. Tensile fault representation has several important geophysical applications, such as modeling of the deformation fields due to dyke injection in the volcanic region, mine collapse and fluid-driven cracks. The strains and stresses within the Earth constitute important precursors of earthquake. Therefore, the calculation of the static and quasi-static deformation of the Earth around surface faults is vital for any scheme for the prediction of earthquakes.

Dislocation theory is very useful to determine the static changes that a company faulting within the earth, which has been discussed by Steketee [14, 15]. As a mathematical model of a fault he used a displacement dislocation surface, i.e., a surface across which there is a discontinuity in the displacement vector. The calculation of the displacement and deformation at a given observation point in different earth models due to slip has a wide range of applications. Many researchers have considered the two half-space model comprising of two half-spaces with different properties separated by a single plane boundary to study the effect of faulting at a material discontinuity such as Singh and Rani [12], Singh et al. [13], Bonafede and Rivalta [2], Kumari et al. [8], Kumar et al. [7], Rani and Bala (2006), Bala and Rani [1], Malik et al. [9, 10], Godara et al. [5, 6] and others. Malik et al.

[10] studied the deformation of two isotropic, homogeneous, perfectly elastic half-spaces in smooth contact caused by a vertical tensile fault. Godara et al. [5] replaced the lower isotropic half-space by the orthotropic half-space and obtained the expressions for stresses and displacements at any point of a two-phase medium consisting of a homogeneous, isotropic, perfectly elastic half-space in smooth contact with a homogeneous, orthotropic, perfectly elastic half-space caused by due to various seismic sources. Godara et al. [6] studied the deformation caused by an inclined dip slip fault of finite width located at an arbitrary distance from the interface in the isotropic half-space. Minakshi et al. [11] considered the same model except the fault type and obtained the expressions for Airy stress function and stresses for both the half-spaces caused by a long inclined tensile fault.

In the present paper, our aim is to obtain the displacement field caused by an inclined tensile fault of finite width located at an arbitrary distance from the interface in the isotropic half-space using the Airy stress function approach. The displacement field due to interface breaking and buried inclined tensile fault has been studied numerically for two orthotropic materials namely Barytes and Topaz. The surface plots for horizontal and vertical displacements are also drawn. It has been observed that variation in depth and dip angle have a significant effect on the variation of horizontal and vertical displacements. The results for an isotropic material, a transversely isotropic material and for a cubic material can be derived as particular cases.

2. Theory

A two-dimensional model consisting of two half-spaces (homogeneous, perfectly elastic that are in smooth contact along the plane $x_3 = 0$) is established. The fault lies entirely in the upper half-space $(x_3 > 0)$ that is isotropic with stress-strain relations;

$$p_{ij} = 2\mu\left[e_{ij} + \frac{\sigma}{1-2\sigma}\delta_{ij}e_{kk}\right], \; (i,\ j = 1,\ 2,\ 3), \tag{1}$$

where p_{ij} are the components of stress tensor, e_{ij} are the components of strain tensor, μ is the shear modulus and σ is Poisson's ratio.

The lower half-space $(x_3 < 0)$ is assumed to be orthotropic with stress-strain relations

$$\begin{bmatrix} p'_{11} \\ p'_{22} \\ p'_{33} \\ p'_{23} \\ p'_{31} \\ p'_{12} \end{bmatrix} = \begin{bmatrix} c_{11} & c_{12} & c_{13} & 0 & 0 & 0 \\ c_{12} & c_{22} & c_{23} & 0 & 0 & 0 \\ c_{13} & c_{23} & c_{33} & 0 & 0 & 0 \\ 0 & 0 & 0 & c_{44} & 0 & 0 \\ 0 & 0 & 0 & 0 & c_{55} & 0 \\ 0 & 0 & 0 & 0 & 0 & c_{66} \end{bmatrix} \begin{bmatrix} e'_{11} \\ e'_{22} \\ e'_{33} \\ 2e'_{23} \\ 2e'_{31} \\ 2e'_{12} \end{bmatrix} \tag{2}$$

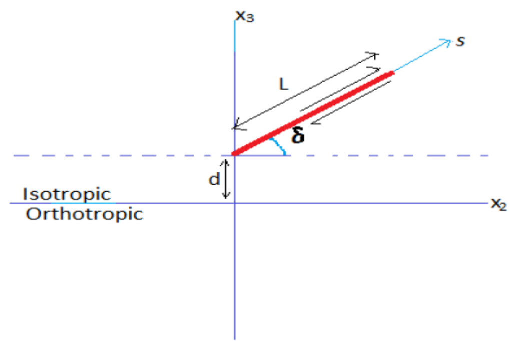

Figure 1. Geometry of a long tensile fault of finite width L having lower edge at a distance d from the interface in the isotropic half-space in smooth contact with an orthotropic half-space where δ is dip angle and s is the distance from the lower edge of the fault, measured in dip direction.

The expressions of Airy stress function and stresses for a long tensile fault of width L and infinite length with lower edge of the fault at distance d from the interface obtained by Minakshi et al. [11] are as follows:

for isotropic half-space,

$$\begin{aligned} U = \frac{\alpha\mu b'}{\pi} & [\{(1 + A_1)\cos^2\delta\}s + (x_2\cos\delta + X\sin\delta - s)\ln R \\ & + \{A_1(x_2\cos\delta - d\sin\delta - s) - x_3\sin\delta)\}\ln S \\ & + 2A_2x_3(x_2\cos\delta - X'\sin\delta - s)(d + s\sin\delta)\frac{1}{S^2} \\ & - x_3\cos\delta(A_1 + 2A_2 - 1)\tan^{-1}\left(\frac{s - x_2\cos\delta + X'\sin\delta}{x_2\sin\delta + X'\cos\delta}\right)]|_0^L \end{aligned} \tag{3}$$

$$
\begin{aligned}
p_{22} = \frac{\alpha\mu b'}{\pi} & [(x_2 \cos\delta + 3X \sin\delta + s\cos 2\delta)\frac{1}{R^2} \\
& - 2(x_2 \cos\delta + X\sin\delta - s)(X - s\sin\delta)^2 \frac{1}{R^4} \\
& + \{2(x_2\cos\delta - X'\sin\delta - s) - (4A_2 + A_1)(x_2\cos\delta + d\sin\delta - s\cos 2\delta) \\
& - x_2 \sin\delta\}\frac{1}{S^2} \\
& - 2\{A_1(x_2\cos\delta - X'\sin\delta - s) - (X' + s\sin\delta)^2 - 2A_2x_3^2\cos\delta(x_2 - s\cos\delta) \\
& -(A_1 - 1)x_3(X' + s\sin\delta)(x_2\cos\delta - X'\sin\delta - s) \\
& + 2A_2(d + s\sin\delta)(X' + s\sin\delta)[2(x_2\cos\delta - X'\sin\delta - s) + 3x_3\sin\delta]\}\frac{1}{S^4} \\
& + 16A_2x_3(x_2\cos\delta - X'\sin\delta - s)(d + s\sin\delta)(X' + s\sin\delta)^2\frac{1}{S^6}]|_0^L
\end{aligned} \tag{4}
$$

$$
\begin{aligned}
p_{23} = \frac{\alpha\mu b'}{\pi} & [-(x_2\sin\delta - X\cos\delta)\frac{1}{R^2} + 2(X - s\sin\delta)^2(x_2\sin\delta - X\cos\delta)\frac{1}{R^4} \\
& + \{-(A_1 + 4A_2 - 1)x_3\cos\delta + (x_2\sin\delta + X'\cos\delta)\}\frac{1}{S^2} \\
& + \{2x_3(A_1 + 2A_2)(X' + s\sin\delta)^2\cos\delta) \\
& -2A_1(X' + s\sin\delta)[X'\cos\delta(X' + s\sin\delta) \\
& + d\sin\delta(x_2 - s\cos\delta) + s\cos\delta(x_2\sin\delta + X'\cos\delta)] \\
& - 4A_2(d + s\sin\delta)[(x_3 + X' + s\sin\delta)(x_2\sin\delta + X'\cos\delta)\}\frac{1}{S^4} \\
& + 2x_3\cos\delta(X' + s\sin\delta)] - 2x_3(X' + s\sin\delta)(x_2\sin\delta + X'\cos\delta)\}\frac{1}{S^4} \\
& + 16A_2x_3(d + s\sin\delta)(X' + s\sin\delta)^2(x_2\sin\delta + X'\cos\delta)\frac{1}{S^6}]|_0^L
\end{aligned} \tag{5}
$$

$$p_{33} = \frac{\alpha\mu b'}{\pi}\left[(x_2\cos\delta - X\sin\delta - s\cos 2\delta)\frac{1}{R^2}\right.$$

$$+ 2(x_2\cos\delta + X\sin\delta - s)(X - s\sin\delta)^2\frac{1}{R^4}$$

$$+ \{A_1(x_2\cos\delta + d\sin\delta - s\cos 2\delta) + x_3\sin\delta\}\frac{1}{S^2}$$

$$+\{2A_1(X' + s\sin\delta)[(X' + s\sin\delta)(x_2\cos\delta - d\sin\delta - s)$$

$$-x_3\cos\delta(x_2 - s\cos\delta)]$$

$$-4A_2x_3[x_3\cos\delta(x_2 - s\cos\delta) + 3\sin\delta(X' + s\sin\delta)(d + s\sin\delta)]$$

$$+ 2x_3(X' + s\sin\delta)(x_2\cos\delta - X'\sin\delta - s)\}\frac{1}{S^4}$$

$$\left. - 16A_2x_3(x_2\cos\delta - X'\sin\delta - s)(d + s\sin\delta)(X' + s\sin\delta)^2\ \right]\Big|_0^L \tag{6}$$

for orthotropic half-space,

$$U^* = \frac{2\alpha\mu b'}{\pi}\left[(B_1 - B_2)s\cos^2\delta - B_2(x_2\cos\delta - d\sin\delta - s)\ln T\right.$$

$$+B_1(x_2\cos\delta - d\sin\delta - s)\ln H$$

$$- B_2ax_3\cos\delta\tan^{-1}\left(\frac{s - x_2\cos\delta + Y\sin\delta}{x_2\sin\delta + Y\cos\delta}\right)$$

$$\left. + B_1bx_3\cos\delta\tan^{-1}\left(\frac{s - x_2\cos\delta + Y'\sin\delta}{x_2\sin\delta + Y'\cos\delta}\right)\right]\Big|_0^L \tag{7}$$

$$p'_{22} = \frac{2\alpha\mu b'}{\pi}\left[-a^2B_2(s\cos 2\delta - x_2\cos\delta - d\sin\delta)\frac{1}{T^2}\right.$$

$$+ b^2B_1(s\cos 2\delta - x_2\cos\delta - d\sin\delta)\frac{1}{H^2}$$

$$+ 2a^2B_2(d + s\sin\delta)(x_2\cos\delta - Y\sin\delta - s)(Y + s\sin\delta)\frac{1}{T^4}$$

$$\left. - 2b^2B_1(d + s\sin\delta)(x_2\cos\delta - Y'\sin\delta - s)(Y' + s\sin\delta)\frac{1}{H^4}\right]\Big|_0^L \tag{8}$$

$$p'_{23} = \frac{2\alpha\mu b'}{\pi}[a^2 B_2 x_3 \cos\delta \frac{1}{T^2} - b^2 B_2 x_3 \cos\delta \frac{1}{H^2}$$

$$+ 2\alpha B_2(d + s\sin\delta)(-x_2 \sin\delta - Y\cos\delta)(Y + s\sin\delta)\frac{1}{T^4}$$

$$- 2bB_1(d + s\sin\delta)(-x_2 \sin\delta - Y'\cos\delta)(Y' + s\sin\delta)\frac{1}{H^4}]|_0^L \tag{9}$$

$$p'_{33} = \frac{2\alpha\mu b'}{\pi}[-B_2(x_2\cos\delta + d\sin\delta - s\cos 2\delta)\frac{1}{T^2}$$

$$+ B_1(x_2\cos\delta + d\sin\delta - s\cos 2\delta)\frac{1}{H^2}$$

$$- 2B_2(d + s\sin\delta)(x_2\cos\delta - Y\sin\delta - s)(Y + s\sin\delta)\frac{1}{T^4}$$

$$+ 2B_1(d + s\sin\delta)(x_2\cos\delta - Y'\sin\delta - s)(Y' + s\sin\delta)\frac{1}{H^4}]|_0^L \tag{10}$$

where now,

$$R^2 = (x_2 - s\cos\delta)^2 + (X - s\sin\delta)^2,\ S^2 = (x_2 - s\cos\delta)^2 + (X' + s\sin\delta)^2,$$

$$T^2 = (x_2 - s\cos\delta)^2 + (Y + s\sin\delta)^2,\ H^2 = (x_2 - s\cos\delta)^2 + (Y' + s\sin\delta)^2,$$

$$X = x_3 - d,\ X' = x_3 + d,\ Y = d - ax_3,\ Y' = d - bx_3,$$

$$f(s)|_0^L = f(L) - f(0).$$

3. Solution of the Problem

The displacements, for the isotropic half-space, are given by the expressions (Singh and Rani [12])

$$2\mu u_2 = -\frac{\partial U}{\partial x_2} + \frac{1}{2\alpha}\int (p_{22} + p_{33})dx_2, \tag{11a}$$

$$2\mu u_3 = -\frac{\partial U}{\partial x_3} + \frac{1}{2\alpha}\int (p_{22} + p_{33})dx_3. \tag{11b}$$

The displacements, for the orthotropic half-space, are given by the expressions (Singh and Rani [12])

$$u_2' = \frac{1}{\Delta}\int (c_{33}p_{22}' + c_{23}p_{33}')dx_2, \tag{12a}$$

$$u_3' = \frac{1}{\Delta}\int (c_{22}p_{33}' - c_{23}p_{22}')dx_3, \tag{12b}$$

where $\Delta = c_{22}c_{33} - c_{23}^2$.

Using equations (3), (4), (6), (11a) and (11b), we will obtain the following expressions of displacements for a long tensile fault of width L and infinite length with lower edge of the fault at distance d from the interface as for isotropic half-space,

$$\begin{aligned} u_2 = \frac{\alpha b'}{2\pi}\Big[\Big[&\left(\frac{1}{\alpha}-1\right)\cos\delta\ln R - \left\{A_1 + \frac{(2A_2-1)}{\alpha}\right\}\cos\delta\ln S \\ &+ \frac{\sin\delta}{\alpha}\left\{\tan^{-1}\left(\frac{x_2 - s\cos\delta}{X - s\sin\delta}\right) - \tan^{-1}\left(\frac{x_2 - s\cos\delta}{X' + s\sin\delta}\right)\right\} \\ &-(X - s\sin\delta)(x_2\sin\delta - X\cos\delta)\frac{1}{R^2} \\ &+\left\{\left(A_1 + \frac{2A_2}{\alpha}\right)(d + s\sin\delta)(x_2\sin\delta + X'\cos\delta)\right. \\ &\left. - x_3[2A_2x_3\cos\delta - (x_2\sin\delta + X'\cos\delta)]\right\}\frac{1}{S^2} \\ &-4A_2x_3(x_2\sin\delta + X'\cos\delta)(d + s\sin\delta)(X' + s\sin\delta)\frac{1}{S^4}\Big]\Big]_0^L \end{aligned} \tag{13}$$

$$\begin{aligned} u_3 = \frac{\alpha b'}{2\pi}\Big[\Big[&\left(\frac{1}{\alpha}-1\right)\sin\delta\ln R - \left(\frac{1}{\alpha}-1\right)\sin\delta\ln\delta \\ &+ \frac{\cos\delta}{\alpha}\left\{\tan^{-1}\left(\frac{X - s\sin\delta}{x_2 - s\cos\delta}\right) + (1-2A_2)\tan^{-1}\left(\frac{X' - s\sin\delta}{x_2 - s\cos\delta}\right)\right\} \\ &+\{A_1 + 2A_2 - 1\}\cos\delta\tan^{-1}\left(\frac{s - x_2\cos\delta + X'\sin\delta}{x_2\sin\delta + X'\cos\delta}\right) \end{aligned}$$

$$- (X - s \sin \delta)(x_2 \cos \delta + X \sin \delta - s) \frac{1}{R^2}$$

$$+ \left\{ \left(-A_1 - 2A_2 + \frac{2A_2}{\alpha} \right) (d + s \sin \delta)(x_2 \cos \delta - X' \sin \delta - s) \right.$$

$$\left. - 2A_2 x_3 (s \cos 2\delta - x_2 \cos \delta - d \sin \delta) - x_3 ((x_2 \cos \delta - X' \sin \delta - s)) \right\} \frac{1}{S^2}$$

$$+ 4A_2 x_3 (x_2 \cos \delta - X' \sin \delta - s)(d + s \sin \delta)(X' + s \sin \delta) \frac{1}{S^4}] |_0^L . \tag{14}$$

Using equations (8), (10), (12a), and (12b), we will obtain the following expressions of displacements for a long tensile fault of width L and infinite length with lower edge of the fault at distance d from the interface as for orthotropic half-space,

$$u_2' = -\frac{2\alpha\mu b'}{\pi} [-B_2 r_1 \cos \delta \ln T + B_1 r_2 \cos \delta \ln H$$

$$+ B_2 r_1 (d + s \sin \delta)(x_2 \sin \delta + Y \cos \delta) \frac{1}{T^2}$$

$$- B_1 r_2 (d + s \sin \delta)(x_2 \sin \delta + Y' \cos \delta) \frac{1}{H^2}] |_0^L \tag{15}$$

$$u_3' = \frac{2\alpha\mu b'}{\pi} [-B_2 s_1 (d + s \sin \delta)(x_2 \cos \delta - Y \sin \delta - s) \frac{1}{T^2}$$

$$+ B_1 s_2 (d + s \sin \delta)(x_2 \cos \delta - Y' \sin \delta - s) \frac{1}{H^2} + B_2 s_1 \cos \delta \tan^{-1} \left(\frac{Y + s \sin \delta}{x_2 - s \cos \delta} \right)$$

$$- B_1 s_2 \cos \delta \tan^{-1} \left(\frac{Y' + s \sin \delta}{x_2 - s \cos \delta} \right)] |_0^L . \tag{16}$$

4. Numerical Results and Discussion

We compare the displacement field due to a long vertical tensile fault of width L its edge at the distance d from the interface located in the isotropic half-space in smooth contact with orthotropic half-space along the horizontal plane of two orthotropic materials namely Barytes and Topaz. We assume the isotropic half-space to be Poissonian so that $\sigma = 0.25$. For the orthotropic half-space, we use the values of elastic constants given by Love (1944). For Topaz,

$$c_{11} = 2870, \quad c_{22} = 3560, \quad c_{33} = 3000$$

$$c_{12} = 1280, \; c_{23} = 900, \; c_{13} = 860,$$

$$c_{44} = 1100, \; c_{55} = 1350, \; c_{66} = 1330.$$

In terms of a unit of 10^6 grammes wt/cm^2, this yields $a = 1.2992$ and $b = 0.8385$. For Barytes,

$$c_{11} = 907, \quad c_{22} = 800, \; c_{33} = 1074,$$

$$c_{12} = 468, \quad c_{23} = 273, \; c_{13} = 275,$$

$$c_{44} = 122, \; c_{55} = 293, \; c_{66} = 283.$$

In terms of a unit of 10^6 grams wt/cm^2, this yields $a = 2.3118$ and $b = 0.3735$.

The results when the lower half-space is also isotropic follow by taking

$$c_{11} = c_{22} = c_{23} = \frac{2\mu'(1-\sigma')}{1-2\sigma'}$$

$$c_{12} = c_{13} = c_{23} = \frac{2\mu'\sigma}{1-2\sigma'}$$

$$c_{44} = c_{55} = c_{66} = \mu'.$$

We take $\sigma' = 0.25$ and $c_{44}/\mu = 0.5$ for numerical computations.

When the lower half-space is cubic, we may take

$$c_{11} = c_{22} = c_{33},$$

$$c_{12} = c_{13} = c_{23},$$

$$c_{44} = c_{55} = c_{66}.$$

The results when the lower half-space is transversely isotropic follow by taking

$$c_{11} = c_{22}, \; c_{13} = c_{23}, \; c_{44} = c_{55},$$

$$c_{66} = \frac{(c_{11} - c_{12})}{2}.$$

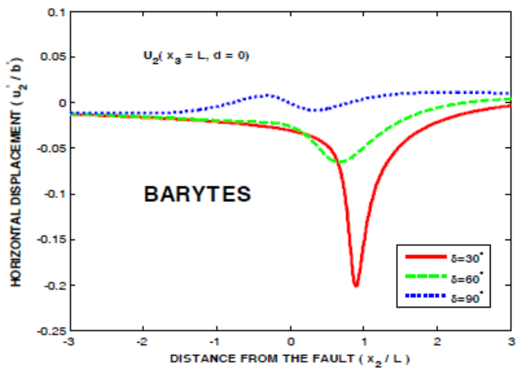

Figure 2(a)

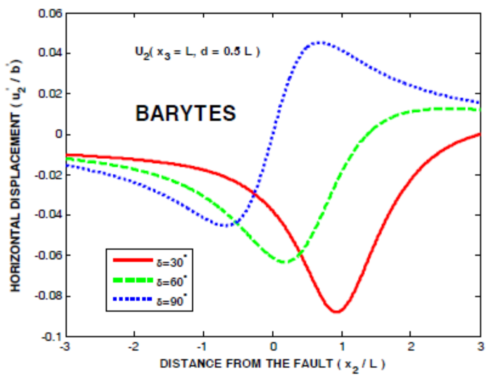

Figure 2(b)

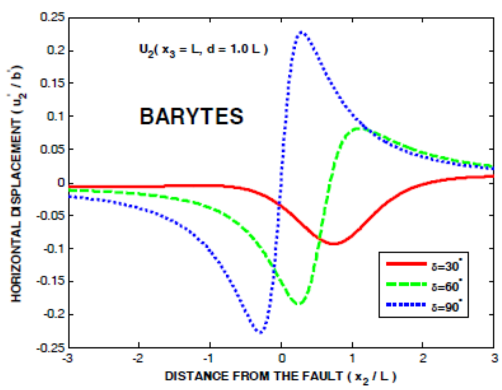

Figure 2(c)

Figure 2. Variation of U_2 versus y.

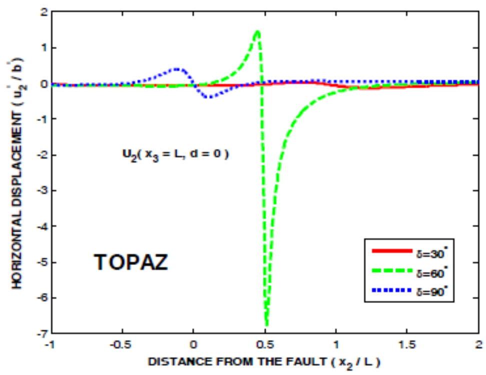

Figure 3(a)

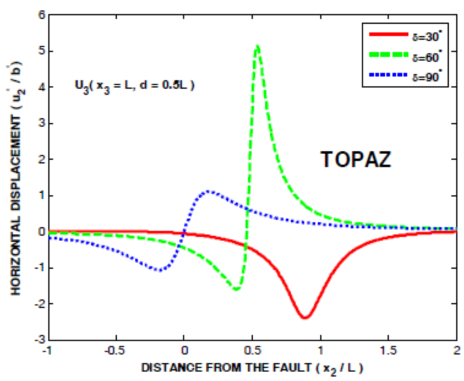

Figure 3(b)

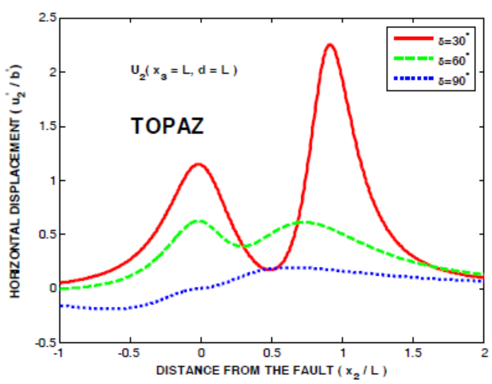

Figure 2(c)

Figure 2. Variation of U_2 versus y.

Figures 2 and 3 display the variation of the horizontal displacement with distance from the fault caused by a tensile fault located in the upper half-space at distance $(a)\, d = 0$, $(b)\, d = 0.5L$ and $(c)\, d = L$ from the interface for dip angles $\delta = 30^\circ$, 60° and 90° for Barytes and Topaz respectively. Here, the observer is in the upper half-space at $x_3 = L$. It is noticed that on moving from interface breaking fault to buried faults, the magnitude of horizontal displacement varies significantly. For Topaz, the horizontal displacement is zero for dip angle 30° for all y. The magnitude of maximum horizontal displacement for Topaz is more than that of Barytes in each case.

In figures 4 and 5, the variation of vertical displacement with respect to distance from the fault is shown. In figure 4(a), for interface breaking fault, the displacement varies abruptly for dip angles 30° and 60°. The pattern and magnitude of displacement varies to a great extent as the value of d increases. The vertical displacement in case of topaz is negligible for dip angle 30° for interface breaking fault $(d = 0)$. In figure 4(a), the discontinuity of vertical displacement exists at $y = 0$ for dip angle 30° while in case of Topaz, the displacement is discontinuous at $y = 0$ and $y = 0.5$ for dip angle 60° for interface breaking fault and at $y = 0$ for buried fault placed at depth $d = 0.5H$ inclined at dip 30°.

Figures 6 and 7 depict the variation of horizontal displacement with depth from the fault for various dip angles for varying d for Barytes and Topaz respectively. Here, the observer is at $x_3 = L$. It is observed that as the dip angle increases, the magnitude of maximum horizontal displacement decreases in each case. The variation of displacement is smooth for all the dip angles and all the values of d. The pattern of variation is not affected as the value of d increases in each case.

In figures 8 and 9, the variation of vertical displacement with depth from the fault is represented. For Topaz, the vertical displacement is negligible near the fault, but as we move away from the fault, U_3 converges from negative to positive values. The pattern of variation of vertical displacement remains unchanged on moving from interface breaking fault to buried faults for each case.

Figures (10)-(13) depict the surface plots of horizontal and vertical displacement due to a vertical tensile fault located at (a) interface breaking fault (b) $d = 0.5L$ (c) $d = L$ for Barytes and Topaz. In figures (10) and (11), as the value of d increases, the horizontal and vertical displacement becomes less pronounced for Baryte. But in case of Topaz, the horizontal displacement is less pronounced and vertical displacement is more pronounced for interface breaking faults than buried faults.

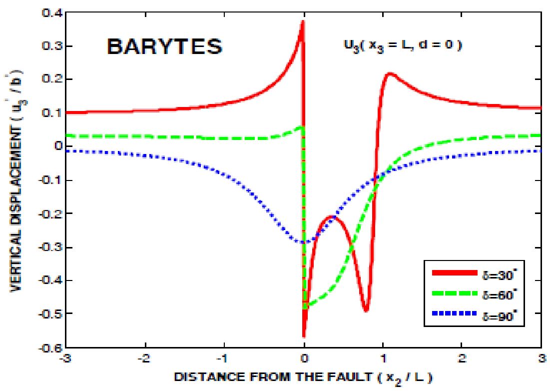

Figure 4(a)

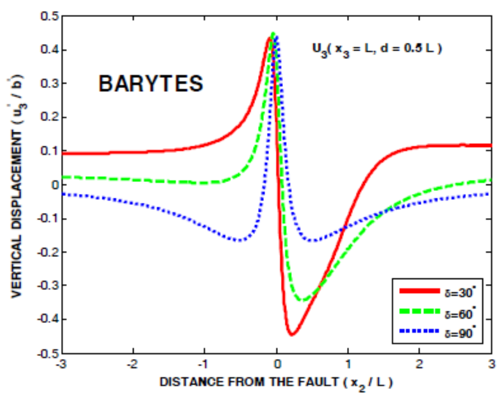

Figure 4(b)

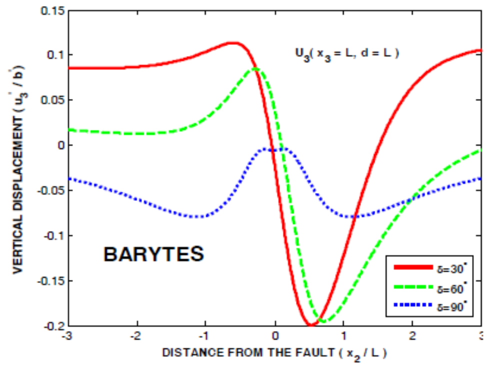

Figure 4(c)

Figure 4. Variation of U_3 versus y.

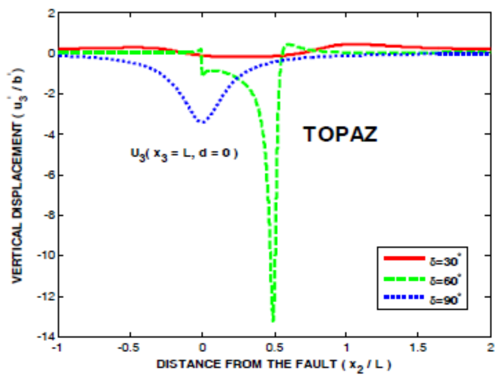

Figure 5(a)

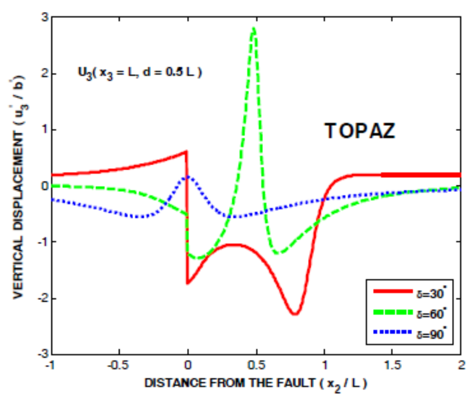

Figure 5(b)

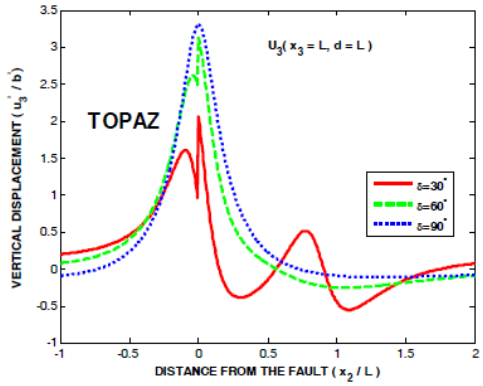

Figure 5(c)

Figure 5. Variation of U_3 versus y.

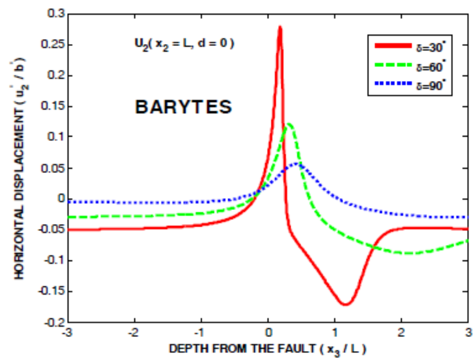

Figure 6(a)

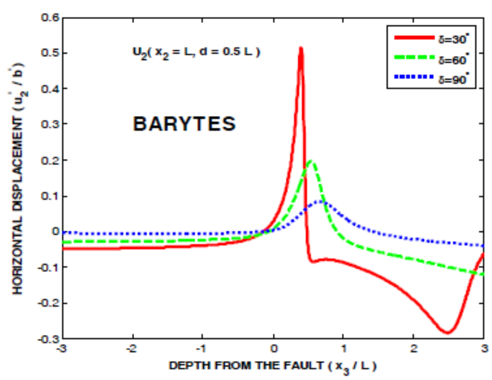

Figure 6(b)

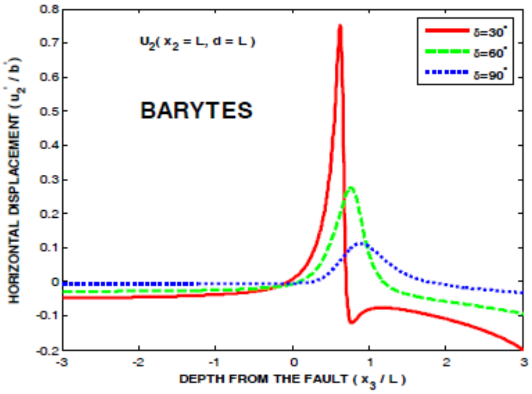

Figure 6(c)

Figure 6. Variation of U_2 versus z.

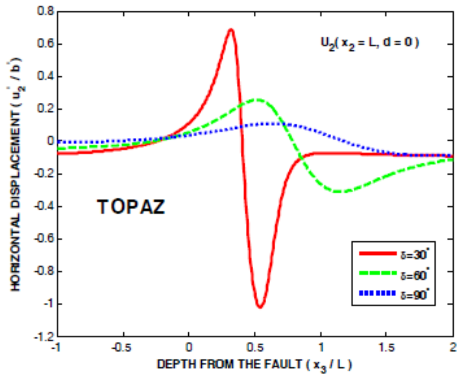

Figure 7(a)

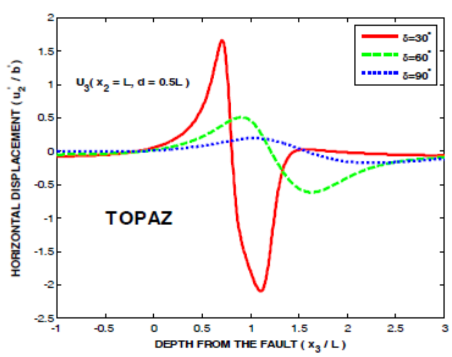

Figure 7(b)

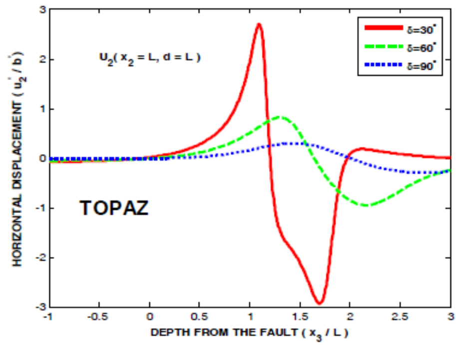

Figure 7(c)

Figure 7. Variation of U_2 versus z.

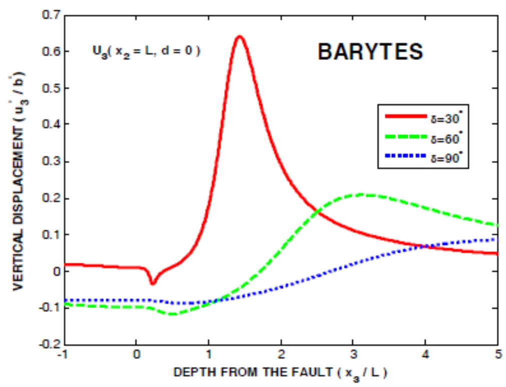

Figure 8(a)

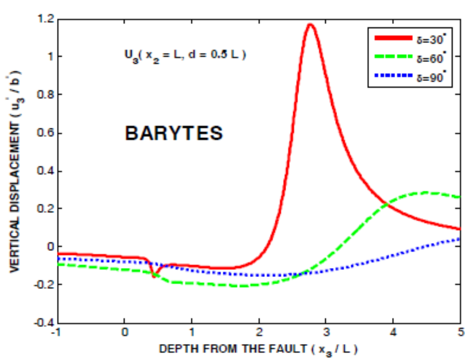

Figure 8(b)

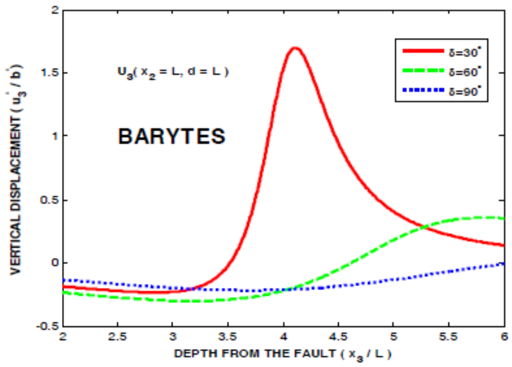

Figure 8(c)

Figure 8. Variation of U_3 versus z.

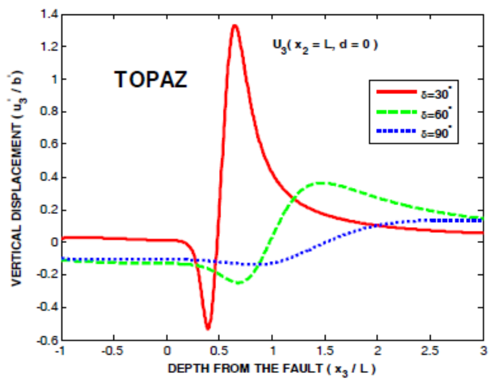

Figure 9(a)

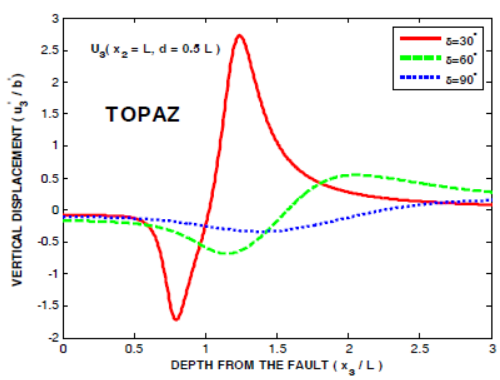

Figure 9(b)

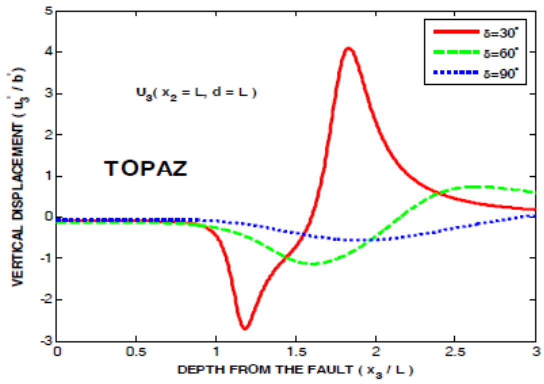

Figure 9(c)

Figure 9. Variation of U_3 versus z.

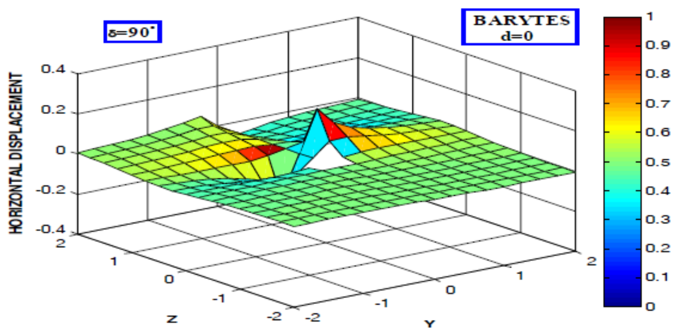

Figure 10(a)

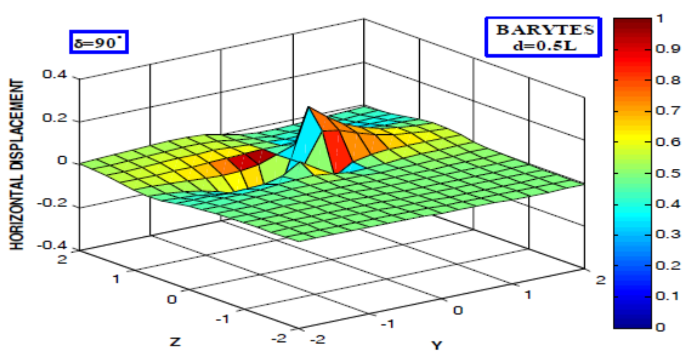

Figure 10(b)

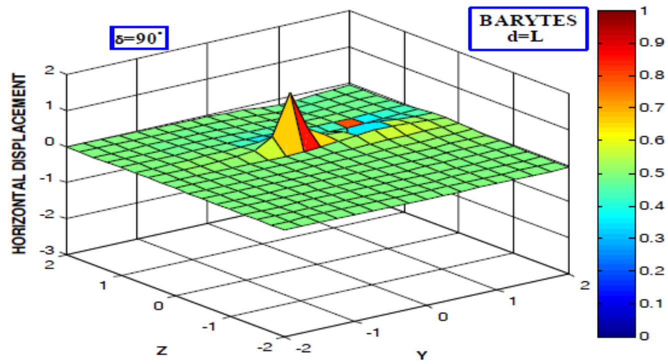

Figure 10(c)

Figure 10. Surface plots for U_2.

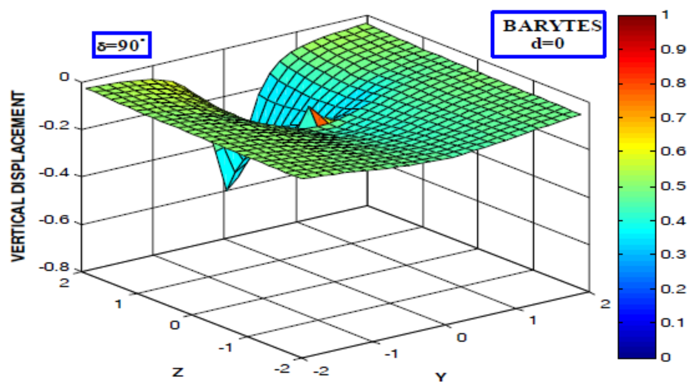

Figure 11(a)

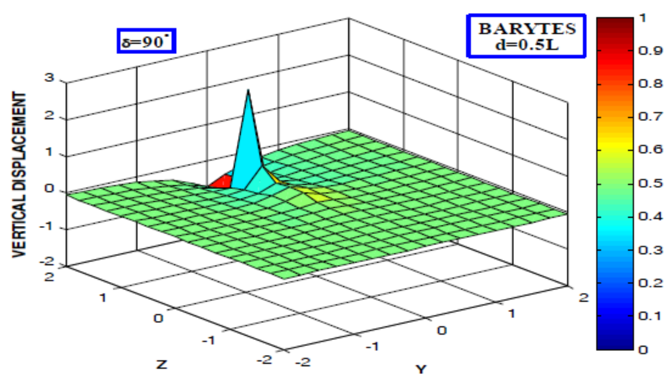

Figure 11(b)

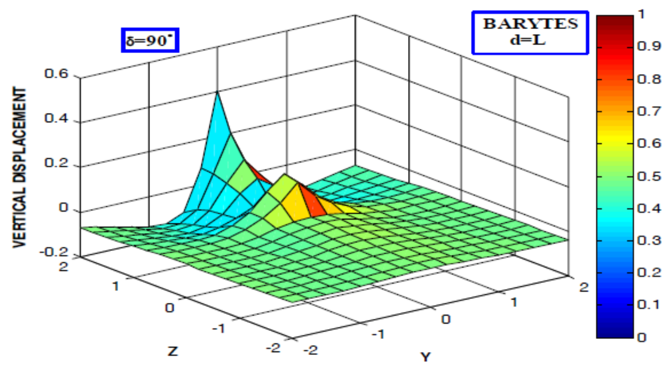

Figure 11(c)

Figure 11. Surface plots for U_2.

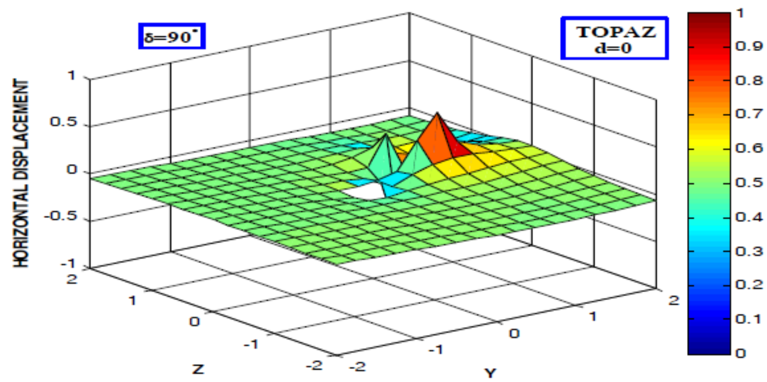

Figure 12(a)

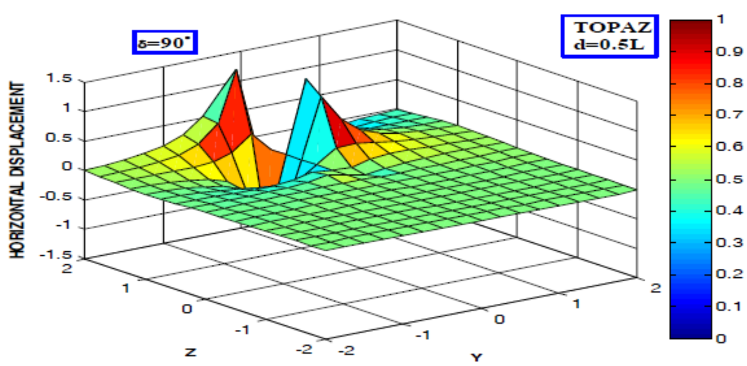

Figure 12(b)

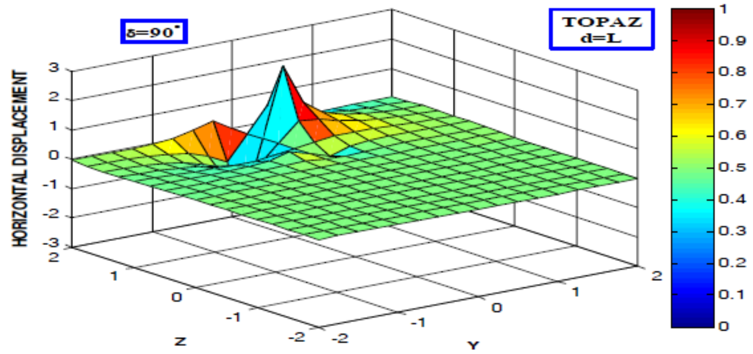

Figure 12(c)

Figure 12. Surface plots for U_2.

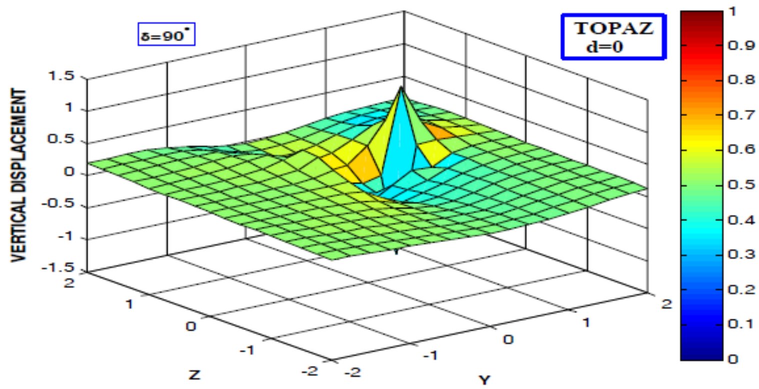

Figure 13(a)

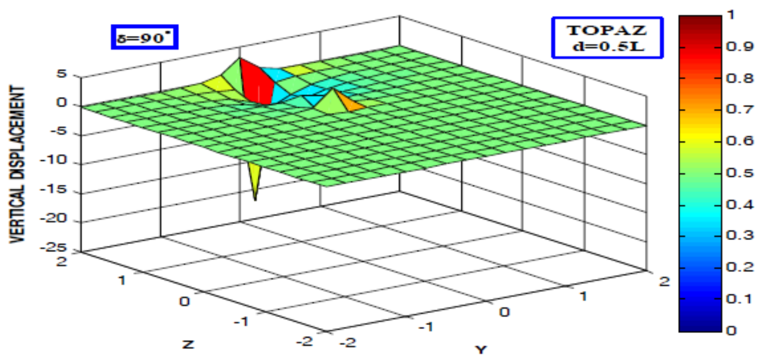

Figure 13(b)

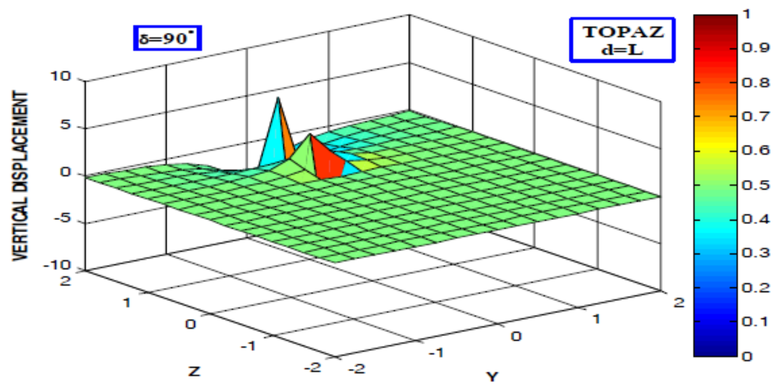

Figure 13(c)

Figure 13. Surface plots for U_3.

6. Conclusion

We have obtained the closed-form expressions for displacements at any point of a two-phase medium consisting of an isotropic half-space overlying the orthotropic half-space due to an inclined tensile fault placed at distance d from the interface in the isotropic half-space. The results obtained satisfy the necessary continuity conditions

$$p_{33} = p'_{33},\ u_3 = u'_3,$$

$$p_{23} = 0,\ p'_{23} = 0$$

at $x_3 = 0$ for two half-spaces in smooth contact along the plane $x_3 = 0$. It has been verified that when the lower half-space is replaced by the isotropic one, then the results of the present paper, in the limit, coincide with the corresponding results of Malik et al. [10] for two half-spaces to be in smooth contact. Numerical computations show that Topaz shows more displacement than Barytes for all the cases. Both the horizontal and vertical displacement tends to zero as y and z approaches to ∞ for the orthotropic materials Barytes and Topaz. Further, there is significant effect of increasing the dip angle on the pattern and magnitude of displacements. Also, the effect of anisotropy is more pronounced in case of Topaz than Barytes. Variation in d results in strong variation in the pattern of displacements w.r.t. distance from the fault in comparison to that of depth from the fault for both the materials. The present study may find application in analysing the deformation field around mining tremors and drilling into the crust of the earth. It may also find application in geophysical engineering problems regarding the deformation of isotropic medium lying over an orthotropic medium.

References

[1] N. Bala and S. Rani, Static deformation due to a long buried dip-slip fault in an isotropic half-space welded with an orthotropic half-space; Sadhana 34 (2009), 887-902.

[2] M. Bonafede and E. Rivalta, On tensile cracks close to and across the interface between two welded elastic half-spaces; Geophys. J. Int. 138 (1999), 410-434.

[3] N. R. Garg et al. Static deformation of an orthotropic multilayered elastic half-space by two-dimensional surface loads; Proc. Ind. Acad. Sci. (Earth Planet. Sci.) 100 (1991), 205-218.

[4] Godara et al. Static deformation due to a long tensile fault of finite width in an isotropic half-space welded with an orthotropic half-space; Bull. Math. Sci. App. 3 (2014), 13-33.

[5] Godara et al. Static deformation due to two-dimensional seismic sources embedded in an isotropic half-space in smooth contact with an orthotropic half-space; Global J. Math. Analysis 2 (2014), 169-183.

[6] Godara et al. Plane strain deformation due to inclined dipping fault in an isotropic half-space in smooth contact with an orthotropic half-space; Advances in Theoretical and Applied Mathematics 11 (2016), 339-360.

[7] A. Kumar et al. Deformation of two welded half-spaces due to a long inclined tensile fault; J. Earth Syst. Sci. 114 (2005), 97-103.

[8] G. Kumari et al. Static deformation of two welded half-spaces caused by a point dislocation source; Phys. Earth. Planet. Inter. 73 (1992), 53-76.

[9] M. Malik et al. Static deformation due to long tensile fault embedded in an isotropic half-space in welded contact with an orthotropic half-space; Inter. J. Sci. Res. Pub. 2 (2012), 1-12.

[10] M. Malik et al. Static deformation of two half-spaces in smooth contact due to a vertical tensile fault of finite width; Inter. J. Comp. 4 (2014), 440-450.

[11] Minakshi, Yogita Godara, Mahabir Singh and Ravinder Kumar Sahrawat, Static deformation due to a long tensile fault of finite width in an isotropic half-space in smooth contact with an orthotropic half-space, Journal of Basic and Applied Engineering Research Volume 5, Issue 5; July-September, 2018, pp. 419-423.

[12] S. Rani and S. J. Singh, Static deformation of two welded half-spaces due to dip-slip faulting; Proc. Ind. Acad. Sci. (Earth Planet. Sci.) 101 (1992), 269-282.

[13] S. J. Singh and S. Rani, Static deformation due to two-dimensional seismic sources embedded in an isotropic half-space in welded contact with an orthotropic half-space; J. Phys. Earth 39 (1991), 599-618.

[14] S. J. Singh et al. Displacements and stresses in two welded half-spaces caused by two-dimensional sources; Phys. Earth Planet. Int. 70 (1992), 90-101.

[15] J. A. Steketee, On Volterra's didlocations in a semi-infinite elastic medium; Can. J. Phys. 36 (1958a), 192-205.

[16] J. A. Steketee, Some geophysical applications of the elasticity theory of dislocations; Can. J. Phys. 36 (1958b), 1168-1198.